

# Cubic interaction parameters for $t_{2g}$ Wannier orbitals

T. Ribic, E. Assmann, A. Tóth, and K. Held

*Institute of Solid State Physics, Vienna University of Technology, A-1040 Vienna, Austria*

(Dated: October 8, 2014)

Many-body calculations for multi-orbital systems at present typically employ Slater or Kanamori interactions which implicitly assume a full rotational invariance of the orbitals, whereas the real crystal has a lower symmetry. In cubic symmetry, the low-energy  $t_{2g}$  orbitals have an on-site Kanamori interaction, albeit without the constraint  $U = U' + 2J$  implied by spherical symmetry ( $U$ : intra-orbital interaction,  $U'$ : inter-orbital interaction,  $J$ : Hund's exchange). Using maximally localized Wannier functions we show that deviations from the standard, spherically symmetric interactions are indeed significant for  $5d$  orbitals ( $\sim 25\%$  for BaOsO<sub>3</sub>;  $\sim 12\%$  if screening is included), but less important for  $3d$  orbitals ( $\sim 6\%$  for SrVO<sub>3</sub>;  $\sim 1\%$  if screened).

PACS numbers: 71.27.+a, 71.10.Fd

## I. INTRODUCTION

Strongly correlated electron systems show a rich variety of unconventional phenomena such as high temperature superconductivity<sup>1</sup> and quantum criticality<sup>2</sup> — and their theoretical description and understanding constitutes a particular challenge. The origin of these correlations is the strong Coulomb interaction, as particularly found in materials with partially filled  $d$ - or  $f$ -bands, such as transition metals, their oxides, rare earth and lanthanide compounds.

The Coulomb interaction between two electrons, which scatter from orbitals  $\alpha$ ,  $\beta$  to  $\alpha'$ ,  $\beta'$  in the course of the interaction, is simply given by

$$U_{\alpha'\beta'\beta\alpha} = \int d^3r d^3r' \psi_{\alpha'}^*(\mathbf{r}) \psi_{\beta'}^*(\mathbf{r}') V(|\mathbf{r}' - \mathbf{r}|) \psi_{\beta}(\mathbf{r}) \psi_{\alpha}(\mathbf{r}). \quad (1)$$

Here,  $V(|\mathbf{r}' - \mathbf{r}|) = e^2 / (4\pi\epsilon_0 |\mathbf{r}' - \mathbf{r}|)$  is the Coulomb interaction with electron charge  $e$  and vacuum permittivity  $\epsilon_0$ ;  $\psi_{\alpha}(\mathbf{r})$  is the electron wave function for orbital  $\alpha$ ; no screening by further electrons has been included in this bare interaction  $U_{\alpha'\beta'\beta\alpha}$ . We do not consider relativistic corrections such as the spin-orbit coupling here so that the one-electron eigenstates simply need to be multiplied with a spinor and the integrals  $U_{\alpha'\beta'\beta\alpha}$  are independent of spin; the  $\alpha'$  and  $\alpha$  one-electron eigenstates (as well as  $\beta'$  and  $\beta$ ) need to have the same spin though.

For practical calculations, it is essential to reduce the number of interaction parameters. Often, e.g. in DFT+ $U$  (density-functional theory augmented by a Hubbard- $U$  interaction in a static mean-field approximation)<sup>3</sup> and DFT+DMFT (dynamical mean-field theory),<sup>4</sup> one considers only the *local* interaction. That is, all orbitals  $\alpha$ ,  $\beta$  in Eq. (1) are on the same site; they might correspond to Wannier orbitals<sup>5</sup> localized around the same lattice site. This is justified not only because this on-site interaction is by far the largest interaction parameter, but also since non-local interactions between orbitals on different sites can be treated in simple (Hartree) mean field theory in the limit of a large number of neighbors.<sup>6</sup> Certainly there

are situations where such non-local interactions can be of importance, particularly in one- and two-dimensions, or also between transition metal  $d$  and oxygen  $p$  orbitals.<sup>7</sup>

A further reduction of parameters can be achieved using the so-called Slater integrals<sup>8</sup>

$$F_l = \int dr dr' R(r)^2 R(r')^2 \frac{\min(r, r')^l}{\max(r, r')^{l+1}} r^2 r'^2. \quad (2)$$

Here, the underlying assumption is spherical symmetry, which allows for an analytical angular integration so that eventually only the integrals Eq. (2) over the radial part  $R(r)$  of the wave functions remain, see Appendix. These Slater integrals, the simpler Kanamori<sup>9</sup> interaction, and or even just a single  $U$ -parameter are commonly used in DFT+ $U$ ,<sup>12?</sup> DFT+DMFT,<sup>4,13,14</sup> or full-multiplet configuration-interaction calculations.<sup>10,11,15</sup> However, a crystal lattice is not spherically symmetric. It has a lower, e.g. cubic, symmetry.

The aim of our paper is hence to analyze the nature and magnitude of the deviations from spherical interaction parameters. To this end, we study the specific and arguably most relevant case of transition metal oxides with a cubic perovskite ( $ABO_3$ ) structure. In Section II, we study analytically the structure of the Coulomb matrix elements for a  $BO_6$  octahedron. For the low energy  $t_{2g}$  orbitals, the cubic Coulomb interaction requires three parameters instead of the two parameters for spherical symmetry. We explicitly derive the most relevant integrals that deviate from the Slater integrals (2).

In Section III, we calculate the quantitative deviations from spherical symmetry by means of maximally localized Wannier orbitals. While the bare interaction in  $3d^1$  SrVO<sub>3</sub> is still described reasonably well by spherically symmetric interaction parameters, the stronger  $p$ - $d$  hybridization in  $5d^4$  BaOsO<sub>3</sub> results in larger deviations ( $\sim 25\%$ ). In a Wannier basis which includes both the transition metal  $t_{2g}$  and the oxygen  $p$  orbitals, working with spherically symmetric interactions is justified. Even for BaOsO<sub>3</sub> deviations between cubic and spherical symmetric interactions are only 3% in this case.

The effect of screening within the Thomas-Fermi approximation is considered in Section III C. For short

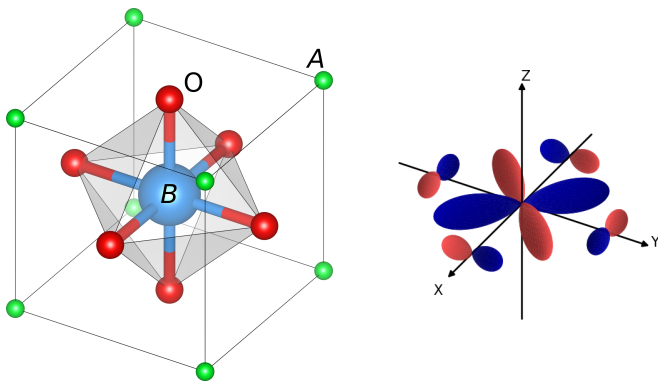


FIG. 1. (Color online.) Left: In the perovskite ( $ABO_3$ ) structure, the oxygen octahedron around the central transition metal ion breaks spherical symmetry down to cubic. The  $B$  ion (large sphere) occupies the center of a cube with  $A$  at the corners and  $O$  at the face centers. Right: Schematic representation of the low energy  $d'_{xy}$  orbital of Eq. (5) [light / dark shading indicates opposite signs of the wave function].

screening lengths, deviations from spherical symmetry are even larger than in the unscreened case; for realistic screening lengths, deviations are reduced but still significant for  $BaOsO_3$  in a 3-orbital Wannier basis ( $\sim 12\%$ ).

## II. CUBIC INTERACTION PARAMETERS

We consider the typical situation for transition metal oxides with an octahedron of oxygens surrounding each transition metal atom as shown in Fig. 1. While an isolated transition metal atom would be spherically symmetric and the parameterization in terms of Slater integrals exact, the oxygen octahedron reduces the symmetry to cubic point group symmetry<sup>16</sup> around the transition metal atom. Therefore, the fivefold degeneracy of the atomic  $d$  level is partially lifted, leaving a threefold degenerate  $t_{2g}$  and a twofold degenerate  $e_g$  level in the cubic environment. In the cases we consider, the octahedron vertices are occupied by negatively charged  $O^{2-}$  ions. In this case, the  $e_g$  states, which have a lot of weight along the  $B$ - $O$  lines, are higher in energy than the  $t_{2g}$  states, whose weight resides predominantly in the space between the  $O$  ions, see Fig. 1 (right).

The effective  $t_{2g}$  orbitals are a combination of predominantly transition metal  $d$  orbitals admixed with oxygen  $p$  orbitals. For many transition metal oxides, these  $t_{2g}$  orbitals constitute the low-energy degrees of freedom for excitations around the Fermi energy.<sup>17</sup> For an analytical description we consider an atomic transition metal  $t_{2g}$  orbital, denoted as  $d_\alpha$  with  $\alpha \in \{xy, yz, xz\}$  in the following. This  $d_\alpha$  orbital mixes with a linear combination of oxygen  $p$  orbitals of the same symmetry, see, e.g., Ref. 11. It is convenient to define this linear combination as  $o_\alpha$ : e.g.,

$$o_{xy} = (p_x^{+y} + p_y^{+x} - p_x^{-y} - p_y^{-x})/2, \quad (3)$$

where  $p_x^{+y}$  is the  $p_x$  orbital centered around the oxygen atom in the the positive  $y$  direction, see Fig. 1. The orbitals  $o_{xz}$  and  $o_{yz}$  follow from Eq. (3) by cubic symmetry, i.e.,  $x \leftrightarrow z$  and  $y \leftrightarrow z$ , respectively.

Symmetry ensures that the orbital  $o_\alpha$  is orthogonal to  $d_{\alpha'}$ , except when  $\alpha = \alpha'$ . Thus to orthogonalize the set of orbitals  $\{o_\alpha, d_{\alpha'}\}$ , one has only to orthonormalize  $o_\alpha$  with respect to its associated  $d_\alpha$ . The orthonormalized orbitals are

$$o'_{\alpha=ij} = \frac{o_{ij} - d_{ij} \langle d_{ij} | o_{ij} \rangle}{\sqrt{1 - \langle d_{ij} | o_{ij} \rangle}}, \quad (4)$$

The mixing of transition metal  $d$  orbitals and oxygen  $p$  orbitals stems from hybridization; by symmetry, there is a hybridization only between  $d_\alpha$  and  $o'_\alpha$  with the same  $\alpha$ . Hence we obtain the tight-binding Hamiltonian

$$\begin{pmatrix} E_d & t \\ t & E_p \end{pmatrix}$$

where  $E_d$  and  $E_p$  are the  $d$  and  $p$  (more precisely the orthogonalized  $o'$ ) energy level;  $E_d - E_p$  is the charge transfer energy. The predominantly  $d$  eigenfunctions of this tight-binding Hamiltonian,  $d'_{ij}$ , are the effective low energy  $t_{2g}$  orbitals

$$d'_{ij} = ad_{ij} + bo'_{ij} \quad (5)$$

with  $\eta = (E_d - E_p)/2t$ ,  $a = [2(\eta^2 - \eta\sqrt{\eta^2 + 1} + 1)]^{-1/2}$ , and  $b = [2(\eta^2 + \eta\sqrt{\eta^2 + 1} + 1)]^{-1/2}$ .

After defining the low energy  $t_{2g}$  orbitals, we need to calculate the Coulomb interaction between these one-particle eigenstates, i.e.,

$$U_{\alpha'\beta'\beta\alpha} = \langle d'_{\alpha'=ij} | \langle d'_{\beta'=kl} | V | d'_{\beta=mn} \rangle | d'_{\alpha=op} \rangle. \quad (6)$$

This is the relevant site-local Coulomb interaction for the low energy degrees of freedom. Note that in this context,  $U_{\alpha'\beta'\beta\alpha}$  is defined as matrix element between direct products of single-particle states denoted as  $|d'_{\beta=mn}\rangle |d'_{\alpha=op}\rangle$ , not between antisymmetrized Fock-states.

Since often  $b \ll 1$  in transition metal oxides, we consider in the following only the leading terms in the limit of large distance between transition metal and oxygen site. In this limit, the direct overlap  $\langle d_{ij} | o_{ij} \rangle$ ,  $b$  (which is the overlap with respect to the one-particle Hamiltonian,  $b \sim t$ ), and Coulomb integrals between orbitals on different sites are small. In the following we hence restrict ourselves to all terms of up to second order in (any) of the above off-site overlaps, and obtain the following three contributions:

Directly from the  $ad_{ij}$  terms in Eq. (5) and from the orthogonalization of the  $o'_{ij}$  we get a contribution

$$(a^4 - 4a^3b \frac{\langle d_{uv} | o_{uv} \rangle}{N}) \langle d_{ij} | \langle d_{kl} | V | d_{mn} \rangle | d_{op} \rangle \quad (7)$$

This term is centered around the transition metal ion and can be expressed in terms of the Slater integrals  $F_l$  for the

$d_{ij}$  orbitals. Hence, this term can still be parameterized with Kanamori interaction parameters.

From two  $bo'_{ij}$ 's in Eq. (5) we get a contribution

$$(2a^2b^2 \frac{1}{N^2}) \langle d_{ij} | \langle o_{kl} | V | o_{mn} \rangle | d_{op} \rangle. \quad (8)$$

Note,  $o_{kl}$  and  $o_{mn}$  have a contribution from the same oxygen site, so that the  $r$  and  $r'$  integrals both include on-site overlaps. Since for large oxygen-transition metal distances the inter-site overlap decays exponentially while the Coulomb interaction decays like  $1/r$ , we keep the term Eq. (8).

Finally, there is a contribution involving only one  $bo'_{ij}$  in Eq. (5) and a Coulomb integral overlap between transition-metal and oxygen site:

$$(2a^3b \frac{1}{N}) \langle d_{ij} | \langle d_{kl} | V | o_{mn} \rangle | d_{op} \rangle. \quad (9)$$

All other terms are of higher order in  $b$  or the off-center overlap integrals.

Eqs. (8) and (9) involve Coulomb integrals with two distinct sites, oxygen and transition metal. Hence, they cannot be expressed in terms of Slater integrals any longer. One can also envisage that from the orbital in Fig. 1 (right). While the spherical rotations around the  $x$  or  $y$  axis of the central  $d_{xy}$  part of the  $d'_{xy}$  orbital in Fig. 1 (right) map the  $d_{xy}$  orbital onto a linear combination of the three  $d_\alpha$  orbitals, this is not possible any longer with the oxygen admixture  $o'_{xy}$  in  $d'_{xy}$  except for 90 degrees rotations. Non-cubic rotations will put the rotated orbitals into positions where there is actually no oxygen site.

Employing the cubic symmetry, we can further reduce the number of integrals needed in Eqs. (7), (8) and (9); or (1) cf. 18. Any integral involving an orbital index  $\alpha = ij$  once or thrice is odd in one cubic direction and hence vanishes. This leaves us with integrals where all orbitals are the same, i.e., the intra-orbital Hubbard interaction  $U = U_{\alpha\alpha\alpha}$  and integrals where we have two distinct orbitals  $\alpha \neq \beta$  twice. For the latter we have the three possibilities: the inter-orbital interaction  $U' = U_{\alpha\beta\beta\alpha}$ , the Hund's exchange  $J = U_{\alpha\beta\alpha\beta}$ , the pair hopping term and  $U_{\alpha\alpha\beta\beta}$  which for real-valued wave functions has the same amplitude as  $J$ . These symmetry considerations actually hold in general, but without spherical symmetry  $U \neq U' + 2J$  because of the terms Eqs. (8) and (9). For spherical symmetry, the connection to the Slater integrals is as follows, cf. 18:  $U = F_0 + \frac{4}{49}(F_2 + F_4)$ ,  $U' = F_0 - \frac{2}{49}F_2 - \frac{4}{441}F_4$ ,  $J = \frac{3}{49}F_2 + \frac{20}{441}F_4$ , so that  $U = U' + 2J$  holds.<sup>19</sup> If we have instead only cubic symmetry, we can still parameterize the interaction in terms of  $U$ ,  $U'$ , and  $J$ , but now with  $U \neq U' + 2J$  and no expression in terms of Slater integrals.

In second quantization, this Kanamori Hamiltonian,<sup>9</sup> which is obtained from Eq.(1) by including all valid spin

combinations in Eq.(1), reads:

$$\begin{aligned} H_U &= \frac{1}{2} \sum_{\substack{\alpha, \beta \\ \alpha', \beta'}} U_{\alpha' \beta' \beta \alpha} \sum_{\sigma, \sigma'} c_{\alpha' \sigma}^\dagger c_{\beta' \sigma'}^\dagger c_{\beta \sigma} c_{\alpha \sigma} \\ &= U \sum_{\alpha} n_{\alpha, \uparrow} n_{\alpha, \downarrow} + \sum_{\substack{\alpha > \beta \\ \sigma, \sigma'}} \left[ (U' - \delta_{\sigma \sigma'} J) n_{\alpha, \sigma} n_{\beta, \sigma'} \right] \\ &\quad - \sum_{\alpha \neq \beta} J (c_{\alpha, \downarrow}^\dagger c_{\beta, \uparrow}^\dagger c_{\beta, \downarrow} c_{\alpha, \uparrow} + c_{\beta, \uparrow}^\dagger c_{\beta, \downarrow}^\dagger c_{\alpha, \uparrow} c_{\alpha, \downarrow} + h.c.). \quad (10) \end{aligned}$$

Here,  $c_{\alpha, \sigma}^\dagger$  ( $c_{\alpha, \sigma}$ ) creates (annihilates) an electron with spin  $\sigma$  in orbital  $\alpha$ ;  $n_{\alpha, \sigma} = c_{\alpha, \sigma}^\dagger c_{\alpha, \sigma}$ .

In contrast for the  $e_g$  orbitals, which are proportional to  $3z^2 - r^2$  and  $\sqrt{3}(x^2 - y^2)$ , the relation  $U = U' + 2J$  still holds for cubic symmetry: Again because of cubic symmetry ( $x \leftrightarrow y$ ) any term involving one or three  $x^2 - y^2$  orbitals vanishes; only the  $U = U_{\alpha\alpha\alpha}$ ,  $U' = U_{\alpha\beta\beta\alpha}$ ,  $J = U_{\alpha\beta\alpha\beta} = U_{\alpha\alpha\beta\beta}$  terms remain. However now, instead of interchanging the orbitals, cubic symmetry operations such as ( $x \rightarrow x, y \rightarrow z, z \rightarrow -y$ ), lead to mixed orbitals:  $3z^2 - r^2 \rightarrow -1/2(3z^2 - r^2) - \sqrt{3}/2\sqrt{3}(x^2 - y^2)$ . Hence, the intra-orbital Hubbard interaction  $U$  for the  $e_g$  orbitals is not a cubic invariant, and  $U$  has to depend on the other parameters  $U'$  and  $J$  through  $U = U' + 2J$ .

### III. QUANTITATIVE DEVIATIONS FOR SrVO<sub>3</sub> AND BaOsO<sub>3</sub>

#### A. Construction of Wannier functions

We now aim to validate our analytical results and quantify the deviation from the spherical-symmetry relation Eq. (1) in real materials. To this end, we perform DFT calculations<sup>20</sup> using a generalized-gradient approximation to the exchange-correlation functional<sup>21</sup> for two cubic perovskite materials, and construct low-energy effective models using maximally-localized Wannier functions (MLWF)<sup>22,23</sup>.

In terms of the formalism of Sec. II, the role of the Wannier functions is to provide the radial dependence of the orbitals which was irrelevant for our arguments from symmetry, but which must be provided to compute numerical values for the interaction parameters. The main difference is that we considered a local octahedron before, while Wannier functions  $|w_{\alpha\mathbf{R}}\rangle$  properly belong to a periodic crystal: they have finite hopping amplitudes  $t_{\alpha\mathbf{R}\alpha'\mathbf{R}'}$  also for  $\mathbf{R} \neq \mathbf{R}'$  (or equivalently, they show a  $\mathbf{k}$ -dispersion), and form an orthonormal set  $\langle w_{\alpha\mathbf{R}} | w_{\alpha'\mathbf{R}'} \rangle = \delta_{\alpha\alpha'} \delta_{\mathbf{R}\mathbf{R}'}$  with respect to sites  $\mathbf{R}$  and orbitals  $\alpha$ .

Our first example is SrVO<sub>3</sub>, which is often used as a ‘‘testbed’’ strongly-correlated material (for DFT+DMFT calculations, see e.g. Ref. 25? ; detailed discussions of Wannier projections in this and related materials have

been given in Refs. 23, 26, and 27). The cubic perovskite  $\text{SrVO}_3$  is a paramagnetic, correlated metal with electronic configuration  $3d^1$ , i.e. one of the  $t_{2g}$ -derived states will be filled.

Secondly, we consider the recently synthesized compound  $\text{BaOsO}_3$ .<sup>28</sup> With a low-spin  $5d^4$  configuration, this is another paramagnetic metal. Since the  $5d$  states are more extended than the  $3d$  states of V, we expect to find greater  $p$ - $d$  hybridization and, in turn, greater deviation from  $U = U' + 2J$  in this case.

For each material, we construct two sets of Wannier functions:

1. three “ $d$ -only” Wannier functions corresponding to the  $d'_{ij}$  of Eq. (5), and
2. twelve “ $d + p$ ” Wannier functions corresponding to the atomic  $d_{ij}$  and  $p_i$  states.

It is instructive to compare these two approaches: The first set of Wannier functions translates the three  $t_{2g}$ -derived bands to three orbitals  $|w'_{\alpha 0}\rangle$  centered on the  $B$  ion. Direct and O-mediated hopping processes are subsumed in an effective  $B$ - $B$  hopping  $t_{d'd'}$ . To account for this, the  $|w'\rangle$  must have substantial weight not only at the  $B$  but also at the O atoms. (In a band picture, the reason is the significant O- $p$  contribution to the  $t_{2g}$ -derived bands.) Which combinations of O- $p$  and  $B$ - $d$  orbitals mix is determined by symmetry as discussed in Sec. II, cf. Fig. 2. Going beyond an effective single-particle description, the Coulomb interaction is expected to be well represented by a site local “multi-band Hubbard” term  $U_{\alpha'\beta'\beta\alpha}$  which can be parameterized by three independent quantities  $U$ ,  $U'$ , and  $J$ , as we saw in the previous section.

The second set of Wannier functions spans nine additional bands, three  $p$ -derived bands per O. With the  $p$ -states explicitly included, the  $d$ -like MLWFs are free to become more localized; the weight at the O sites will be carried by the  $p$ -like orbitals (cf. Fig 3). The downside is that the resulting model becomes significantly more complex, since a correct treatment of such a “ $d + p$ ” model must take into account not only the intra-atomic interactions on the  $B$  ( $U_{dd}$ ) and on the O ( $U_{pp}$ ) sites, but also inter-atomic ( $U_{pd}$ ) interactions.<sup>7,29</sup> This added complexity will increase the computational cost to solve the model in any numerical method, but it will also make the physical interpretation of the results more involved.

Before we turn to the results, note that the heavy ( $Z = 76$ ) element Os leads to an appreciable spin-orbit splitting in  $\text{BaOsO}_3$ . Because it would invalidate the symmetry analysis of Sec. II, we neglect this effect in the construction of the Wannier functions. While our analysis could be extended to include spin-orbit coupling, a spin-orbit interaction term can also be added to the tight-binding model afterwards in any case<sup>30</sup>.

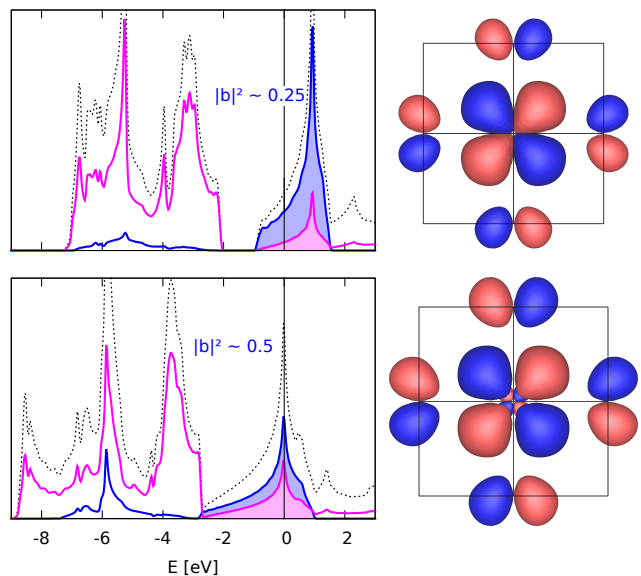


FIG. 2. (Color online.) Densities of states and Wannier functions for the “ $d$ -only” Wannier orbitals for  $\text{SrVO}_3$  (top) and  $\text{BaOsO}_3$  (bottom). On the left, we show the total DOS (dotted line), and the projections on transition-metal  $t_{2g}$  (dark) and O (light) states. The shaded area marks the region of integration used to estimate the O- $p$  weight [corresponding to  $|b|^2$  in Eq. (5)], see text. On the right, the light / dark lobes are isosurfaces for the positive / negative parts of the real-valued Wannier functions. The strong  $p$ - $t_{2g}$  hybridization and the antibonding character are plainly visible.

## B. Results

Fig. 2 shows the densities of states (DOS) of  $\text{SrVO}_3$  and  $\text{BaOsO}_3$ , and the Wannier orbitals corresponding to the 3-band case. The DOS around the Fermi level is derived from the  $\pi$ -antibonding combinations of O- $p$  and  $B$ - $t_{2g}$  states; correspondingly, the 3-band orbitals are composed of a  $d$ -like contribution at the  $B$  site and  $p$ -like contributions at the O sites sharing a plane with the  $d$ -like part, akin to the  $o'_\alpha$  orbitals in Section II. These Wannier orbitals are also referred to as “ $d$ -only”, where the quotation marks hint that these orbitals are actually not pure  $d$ -orbitals. The Wannier functions are equivalent to each other under cubic symmetry.

As expected, the  $p$ - $d$  hybridization is stronger in  $\text{BaOsO}_3$  than  $\text{SrVO}_3$ . This is seen both in the DOS (more O weight around the Fermi energy  $E_F = 0$ ) and in the orbitals (bigger lobes at the O sites). We can quantify this observation by integrating over the shaded areas in the DOS; this yields an O admixture of  $|b_{\text{SrVO}_3}|^2 \sim 0.25$  and  $|b_{\text{BaOsO}_3}|^2 \sim 0.5$ , respectively. In this sense, the “ $d$ -bands” of  $\text{BaOsO}_3$  consist in fact of almost equal parts O and Os contributions. These values agree qualitatively with Eq. 5, which yields  $|b_{\text{SrVO}_3}|^2 \sim 0.20$  and  $|b_{\text{BaOsO}_3}|^2 \sim 0.33$  using the parameters from Table VI.<sup>31</sup> Quantitative differences have to be expected because (i) Eq. (5) holds for an isolated octahedron instead of the

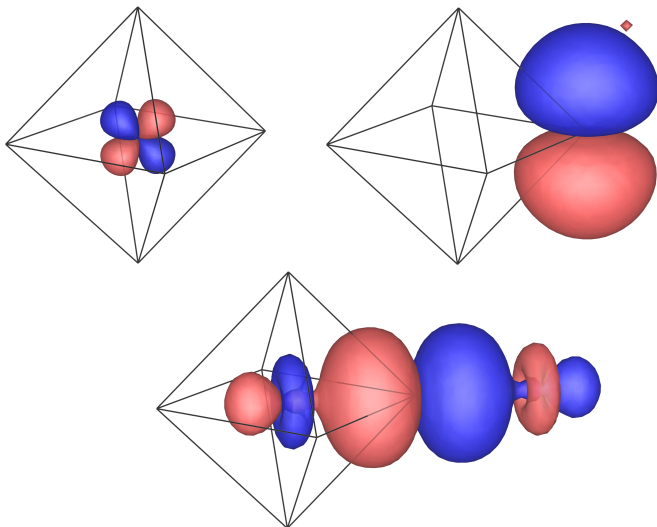


FIG. 3. (Color online.) 12-orbital Wannier functions for  $\text{SrVO}_3$  (plotted as in Fig. 2 right). By symmetry, the twelve orbitals are grouped into three equivalent  $d$ -like orbitals (top left); and two types of  $p$ -like orbitals, three “ $p_\sigma$ ” (bottom) whose symmetry axes point toward their  $B$  neighbors, and six “ $p_\pi$ ” (top right) pointing away from the  $B$  sites. With the O- $p$  states explicitly included, no  $p$ - $t_{2g}$  hybridization is seen in these orbitals. Correspondingly, the  $d$  and  $p_\pi$  orbitals are close to their atomic counterparts. Conversely, the  $p_\sigma$  orbitals, which mediate the  $\sigma$ -bonding between O- $p$  and  $B$ - $e_g$  states, are elongated along their symmetry axis and have large contributions at their  $B$  neighbors.<sup>26,27</sup>

TABLE I. Coulomb interactions (unscreened) for “ $d$ -only” Wannier functions of  $\text{SrVO}_3$  and  $\text{BaOsO}_3$ ;  $(U - U')/2 = J$  holds for spherical but not for cubic symmetry, for  $\text{BaOsO}_3$  deviations are indeed substantial.

interaction	$\text{SrVO}_3$	$\text{BaOsO}_3$
$U$	16.30 eV	10.54 eV
$U'$	15.14 eV	9.67 eV
$J$	0.55 eV	0.33 eV
$(U - U')/2$	0.58 eV	0.44 eV

periodic crystal, (ii) there are further hopping integrals that would have to be considered, and (iii) the partial DOS of Fig. 2 are only projections within the muffin tin spheres<sup>20</sup>.

For these “ $d$ -only” Wannier orbitals, we have calculated the Coulomb interaction by spatial integration of Eq. (1).<sup>32</sup> Table I summarizes the results obtained for the bare interaction. For the  $3d^1$  perovskite  $\text{SrVO}_3$ , deviations from the spherical symmetric relation  $U - U' = 2J$  are 6%. That is, calculations employing this relation can still be expected to yield quite reliable results. For the  $5d^4$  perovskite  $\text{BaOsO}_3$ , on the other hand, deviations are 25%. The reason for this is the larger admixture of oxygen  $p$  contributions, which according to Section II yields larger off-center Coulomb integral overlaps and hence a larger deviation from spherical symmetry.

Recently, transition metal oxides with heavy  $4d$  or  $5d$  elements attract more and more attention. Indeed in such systems electronic correlations are stronger than expected – due to Hund’s rule coupling<sup>18,33,35</sup>. All the more important is a correct Hamiltonian and multiplet structure with Hund’s exchange. In this respect, our finding highlights the substantial difference between  $(U - U')/2$  and  $J$ . A Kanamori Hamiltonian with three independent Coulomb interactions needs to be considered for obtaining the correct multiplet structure.

Next, we turn to the 12-orbital “ $d + p$ ” Wannier functions. This is an alternative description of the low energy physics, where the oxygen  $p$ -orbitals are explicitly taken into account. The corresponding Wannier functions for  $\text{SrVO}_3$  are shown in Fig. 3. The  $d$ -like orbitals are again equivalent up to symmetry, but two inequivalent types of  $p$ -like orbitals appear. Symmetry also greatly restricts the possible hopping processes between these states. The hopping amplitudes within the octahedron as well as selected longer-ranged ones for all four Wannier projections are reported in App. B.

We list the Coulomb interaction parameters between the 12-band orbitals for  $\text{SrVO}_3$  and  $\text{BaOsO}_3$  in Tables II and III, respectively. For the  $d$ -like orbitals,  $U = U' + 2J$  is fulfilled with a reasonable accuracy of 3% even in  $\text{BaOsO}_3$ . Having the additional degree of freedom regarding oxygen- $p$  Wannier orbitals, the  $t_{2g}$  orbitals are now localized around the transition metal ion and have the spherically symmetric form, cf. Fig. 3. In this case, two parameters are sufficient for the  $d$ - $d$  Kanamori interaction.

As a side note, observe that in the 12-band case  $U - U' < 2J$ , while in the 3-band case  $U - U' > 2J$ . This is because  $U'$  and  $J$  are more strongly reduced than  $U$  by the shift of  $t_{2g}$  weight to the oxygens which occurs in the 3-band case, as  $U'$  and  $J$  are *inter*-orbital interactions that include more non-overlapping oxygens in the interaction integral.

Let us emphasize that the  $d$ - $p$  interaction also plays an important role<sup>29</sup>. The  $d$ - $p$  interactions of density-density type are listed in Tables II and III (right). There are two types of  $p$  orbitals, denoted as  $p_\pi$  and  $p_\sigma$  (see Fig. 3). Interactions with  $p$  orbitals centered on an oxygen atom outside the plane of the  $d$  orbital lobes are denoted by  $\perp$ . The  $d$ - $p_\sigma$  interactions  $U_{p_\sigma d}$  and  $U_{p_\sigma d}^\perp$  with the  $p_\sigma$  orbitals oriented toward the transition metal site is considerably stronger than that with the more regular  $p_\pi$  orbitals. There is only one  $U_{p_\pi d}^\perp$ , while two parameters arise from density-density interaction between  $d$  and  $p_\pi$  orbitals with the  $p_\pi$  orbitals being centered around oxygen sites within the plane defined by the  $d$  orbitals. We denote these as  $U_{p_\pi d}$  if the  $p_\pi$  orbital lies within the same plane and  $U_{p_\pi d}'$  if it is oriented perpendicular to it. The considerable differences in the  $d$ - $p$  Coulomb interaction can be understood from the very different  $p_\pi$  and  $p_\sigma$  orbitals in Fig. 3. These differences are of relevance for  $d + p$  DFT+DMFT calculations that include  $U_{pd}$ .<sup>29</sup>

TABLE II. Left: Same as Table I but for  $d+p$  SrVO<sub>3</sub> Wannier functions. Right: the different  $d-p$  density-density Coulomb interactions for these Wannier functions, see main text for the notation.

interaction	SrVO <sub>3</sub>	interaction	SrVO <sub>3</sub>
$U$	19.99 eV	$U_{p\pi d}$	7.24 eV
$U'$	18.52 eV	$U'_{p\pi d}$	7.18 eV
$J$	0.74 eV	$U_{p\sigma d}$	8.52 eV
		$U_{p\sigma d}^\perp$	6.87 eV
		$U_{p\pi d}^\perp$	8.06 eV
$(U - U')/2$	0.74 eV		

TABLE III. Same as Table II but for  $d + p$  BaOsO<sub>3</sub> Wannier functions.

interaction	BaOsO <sub>3</sub>	interaction	BaOsO <sub>3</sub>
$U$	14.90 eV	$U_{p\pi d}$	6.94 eV
$U'$	13.65 eV	$U'_{p\pi d}$	6.80 eV
$J$	0.64 eV	$U_{p\sigma d}$	7.85 eV
		$U_{p\sigma d}^\perp$	7.23 eV
		$U_{p\pi d}^\perp$	6.38 eV
$(U - U')/2$	0.62 eV		

### C. Effect of screening

The values reported above were calculated for a bare, unscreened Coulomb interaction. In this section we include screening, within Thomas-Fermi theory. That is, we replace the bare interaction in Eq. (1) by

$$V(|\mathbf{r}' - \mathbf{r}|) = \frac{e^2}{4\pi\epsilon_0} \frac{1}{|\mathbf{r}' - \mathbf{r}|} e^{-|\mathbf{r}' - \mathbf{r}|/\lambda_{\text{TF}}}, \quad (11)$$

where  $\lambda_{\text{TF}}$  is the Thomas-Fermi screening length. Let us emphasize that for a cubic crystal the screened interaction  $V(\mathbf{r}, \mathbf{r}')$  itself will be of cubic symmetry, and hence deviate from spherical symmetry. This effect is not taken into account in the following; it will on its own generate further deviations of the Kanamori interaction parameters from the spherical relation  $U = U' + 2J$ .

In the following, we adjust the parameter  $\lambda_{\text{TF}}$  to yield a screened Coulomb interaction  $U' \sim 3.5$  eV for  $3d$  SrVO<sub>3</sub> as calculated by constrained LDA<sup>25?</sup>. This corresponds to a screening length  $\lambda_{\text{TF}} = 0.43\text{\AA}$  (the lattice parameters are  $a_{\text{SrVO}_3} = 3.8425\text{\AA}$ <sup>36</sup> and  $a_{\text{BaOsO}_3} = 4.025\text{\AA}$ <sup>28</sup>). We employ the same screening length also for BaOsO<sub>3</sub> as this yields an interaction parameter  $U' \sim 1.8$  eV, which is in the expected range for the  $5d$  BaOsO<sub>3</sub>.

Table IV shows the results obtained for the “ $d$ -only” models. In the case of  $3d$  orbitals as exemplified by SrVO<sub>3</sub>, deviations from spherically symmetric interaction parameters are already small without screening and become negligible if screening is included. By contrast, for  $5d$  BaOsO<sub>3</sub>,  $U - U' = 2J$  is significantly violated even when screened. Let us note that the degree of deviation is quite robust over a large range of screening lengths. For example with  $\lambda_{\text{TF}} = 0.61\text{\AA}$  we obtain a similar deviation of 14% ( $U = 2.55$  eV,  $U' = 1.90$  eV, and  $J = 0.28$  eV).

Interestingly, for weak screening (large  $\lambda$ )  $J$  can even

TABLE IV. Same as Table I but for screened interaction with screening length  $\lambda_{\text{TF}} = 0.43\text{\AA}$ .

interaction	SrVO <sub>3</sub>	BaOsO <sub>3</sub>
$U$	4.40 eV	2.44 eV
$U'$	3.47 eV	1.80 eV
$J$	0.46 eV	0.28 eV
$(U - U')/2$	0.47 eV	0.32 eV

be enhanced whereas  $U$  and  $U'$  are always reduced. The reason for this is that the exchange integral  $J$  includes positive *and* negative contributions; and for large  $\lambda_{\text{TF}}$ , the negative contributions are more strongly reduced than the positive ones. For example at  $\lambda_{\text{TF}} = 21.13\text{\AA}$  we obtain  $J = 0.5465$  eV for SrVO<sub>3</sub>, which is larger than the unscreened  $J = 0.5464$  eV. As the increase is very small, the results are given to a higher precision than elsewhere in the paper. With  $U = 15.67$  eV and  $U' = 12.50$  eV, deviations are 6.2% for this screening strength.

In the limit of infinite screening, i.e.,  $\lambda_{\text{TF}} \rightarrow 0$ , one can show that  $U' = J$ . That is, one can describe this limit by one Kanamori interaction parameter  $U = 3U' = 3J$  for spherical symmetry, and two ( $U$  and  $U' = J$ ) for cubic symmetry. Numerically, we get however also for cubic “ $d$ -only” Wannier functions  $U/J \sim 3$  for both SrVO<sub>3</sub> and BaOsO<sub>3</sub>. The limits of strong and weak screening show that the idea that screening strongly reduces  $U'$  and hardly reduces  $J$  is not true in general. For strong screening,  $J$  is reduced as much as  $U'$ , since they are equal, while for weak screening  $J$  is even enhanced.

## IV. CONCLUSION

We have analyzed the physical origin and the magnitude of the difference between a spherically symmetric and a cubic interaction for  $t_{2g}$  orbitals. Deviations are quite large for  $5d$  orbitals of heavy transition metals. Since for these systems Hund’s exchange is paramount for electronic correlations,<sup>18</sup> we conclude that a Kanamori interaction with three instead of two independent parameters is necessary. Unfortunately, this requires the calculation of one additional interaction parameter and hence a more thorough analysis of the interaction in DFT+DMFT calculations than customary hitherto. Only if the oxygen degrees of freedom are included in the Wannier projection, this is not necessary. In this case, however, the (different)  $d-p$  Coulomb interactions should be taken into account. For  $e_g$  orbitals there is no such difference between spherical and cubic interaction.

Depending on the screening length, screening enhances or reduces the difference between spherically symmetric and cubic interaction parameters. Screening can even enhance  $J$  whereas  $U$  and  $U'$  are always reduced. For Thomas-Fermi screening,  $U = U' + 2J$  is still significantly violated for  $5d$  BaOsO<sub>3</sub>. Let us note that the



simple Thomas-Fermi screening employed here is spherically symmetric, whereas the physical screening function obeys the cubic, not the spherical symmetry. This effect is an additional source of deviations from spherically symmetric interaction parameters.

For both  $e_g$ -only and  $t_{2g}$ -only low-energy effective models, we have a Kanamori interaction for cubic symmetry. This makes continuous-time quantum Monte-Carlo simulations<sup>37</sup> very efficient because of an additional local symmetry, see Ref. 38.

## ACKNOWLEDGMENTS

This work has been supported by the European Research Council under the European Union's Seventh

Framework Programme (FP/2007-2013)/ERC through grant agreement n. 306447; and by an *innovative project* grant from Vienna University of Technology (EA).

## Appendix A: Coulomb interaction and Slater integrals

For the sake of completeness, let us briefly add the representation of the Coulomb interaction Eq. (1) by Slater integrals. Expressing  $1/|\mathbf{r} - \mathbf{r}'| = \sum_{l,m} \frac{\min(r, r')^l}{\max(r, r')^{l+1}} \frac{4\pi}{2l+1} Y_{l,m}(\theta, \varphi) Y_{l,m}^*(\theta', \varphi')$  in terms of spherical harmonics  $Y_{l,m}$  and with  $\psi_\alpha(\mathbf{r}) = R(r)Y_\alpha$  where  $R(r)$  is independent of  $l$  (or  $\alpha$ ), the Coulomb interaction Eq. (1) becomes

$$U_{\alpha'\beta'\beta\alpha} = \frac{e^2}{4\pi\epsilon_0} \int dr d\Omega dr' d\Omega' R(r)Y_{\alpha'}(\theta, \varphi) R(r')Y_{\beta'}(\theta', \varphi') \sum_{l,m} \left[ \frac{\min(r, r')^l}{\max(r, r')^{l+1}} \frac{4\pi}{2l+1} Y_{l,m}(\theta, \varphi) Y_{l,m}(\theta', \varphi') \right] R(r')Y_{\beta}(\theta', \varphi') R(r)Y_{\alpha}(\theta, \varphi) r'^2 r^2. \quad (\text{A1})$$

TABLE V. Hopping amplitudes  $t$  between the three  $t_{2g}$  Wannier functions at various distances, and their on-site energies  $E$  relative to the Fermi level. Values are in eV.

	$t_\pi^{(1)}$	$t_\delta^{(1)}$	$t_\sigma^{(2)}$	$t_\perp^{(2)}$	$t_\parallel^{(2)}$	$E$
SrVO <sub>3</sub>	-0.263	-0.027	-0.084	0.009	0.006	0.580
BaOsO <sub>3</sub>	-0.394	-0.043	-0.112	0.012	0.013	-0.453

This integral can be decomposed into a radial ( $drdr'$ ) and an angular part ( $d\Omega d\Omega'$ ), and the latter can be expressed in terms of Clebsch-Gordan coefficients. Thus only the radial integrals aka Slater parameters  $F_l$  of Eq. (2) need to be calculated.

## Appendix B: Hopping matrices

In this Appendix, we report the numerical values of selected hopping amplitudes in our Wannier projections.<sup>39</sup> The values for SrVO<sub>3</sub> may be compared to Refs. 23 and 26. Note that this is not an enumeration of the largest hopping amplitudes; rather, the selection is meant to be illustrative.

For the 3-band Wannier functions (values in Table V), no hopping is possible within the unit cell. Two nearest-neighbor hoppings are allowed, a  $\pi$ -type hopping  $t_\pi^{(1)}$  when the displacement is in the same plane as the orbital lobes (e.g.  $xy$  orbitals with displacement (100)),

and a smaller  $t_\delta^{(1)}$  of  $\delta$  type where the displacement is perpendicular (e.g.  $xy$  and (001)). Inter-orbital nearest-neighbor hopping is forbidden by cubic symmetry. There are three second-nearest neighbor hopping parameters:  $t_\sigma^{(2)}$  when both orbitals and the displacement share a plane (e.g.  $xy$  and (110));  $t_\parallel^{(2)}$  when the orbitals' planes are parallel (e.g.  $xz \leftrightarrow xz$  and (110)); and  $t_\perp^{(2)}$  when the planes are perpendicular (e.g.  $xz \leftrightarrow yz$  and (110)).

For the 12-band case (Table VI), we report the nearest-neighbor  $d \leftrightarrow d$  hopping parameters  $t_{dd}^{(1)}$  analogous to those of the 3-band case, but not those to further neighbors. In any case, O-mediated hopping, which was subsumed in the hoppings of the 3-band orbitals, now has to be taken into account explicitly.

Within the octahedron, the following hopping processes are possible:  $t_{dp_\pi}$  when the  $p_\pi$  orbital resides in the plane defined by the  $d$  (e.g.  $d_{xy} \leftrightarrow p_y^{+x}$ );  $t_{p_\pi p_\pi}$  between nearest O neighbors, i.e. along an edge of the octahedron (e.g.  $p_y^{+x} \leftrightarrow p_y^{+z}$ );  $t_{p_\pi p'_\pi}$  which is the same as the last, but between orbitals of different orientation (e.g.  $p_y^{+x} \leftrightarrow p_x^{+y}$ );  $t_{p_\pi p_\sigma}$  along an edge (e.g.  $p_y^{+x} \leftrightarrow p_y^{+y}$ );  $t_{p_\sigma p_\sigma}$  along an edge (e.g.  $p_x^{+x} \leftrightarrow p_y^{+y}$ );  $t_{p_\pi p_\pi}^{(1)}$  across the octahedron (e.g.  $p_y^{+x} \leftrightarrow p_y^{-x}$ ); and  $t_{p_\sigma p_\sigma}^{(1)}$  across the octahedron (e.g.  $p_x^{+x} \leftrightarrow p_x^{-x}$ ).

Comparing the sequences of values for the two materials, the same trends are observed (with the exceptions of  $t_\perp^{(2)} \geq t_\parallel^{(2)}$  and  $|t_{p_\pi p_\pi}| \geq |t_{p_\sigma p_\sigma}|$ ). However, the values for the “ $d$ -only” orbitals, and for  $dd$  and  $pd$  processes in the

TABLE VI. Selected hopping amplitudes  $t$  between 12-band Wannier functions, and their on-site energies  $E$  relative to the Fermi level. Where the sign of the hopping alternates due to the signs of the  $p$ -type orbitals, we give the modulus. Values are in eV.

	$t_{dd\pi}^{(1)}$	$t_{dd\delta}^{(1)}$	$ t_{dp\pi} $	$ t_{p\pi p\pi} $	$ t_{p\pi p'_\pi} $	$ t_{p\pi p\sigma} $	$t_{p\sigma p\sigma}$	$t_{p\pi p\pi}^{(1)}$	$t_{p\sigma p\sigma}^{(1)}$	$E_d$	$E_{p\pi}$	$E_{p\sigma}$
SrVO <sub>3</sub>	-0.128	-0.005	1.099	0.064	0.369	0.258	-0.044	-0.078	0.671	-0.407	-3.780	-5.520
BaOsO <sub>3</sub>	-0.187	-0.002	1.240	0.007	0.204	0.195	-0.024	-0.107	0.903	-2.063	-3.896	-6.887

12-band orbitals, are in general larger for BaOsO<sub>3</sub> than SrVO<sub>3</sub>, the larger lattice constant of BaOsO<sub>3</sub> notwithstanding (4.03 Å versus 3.84 Å for SrVO<sub>3</sub>). This is reflective of the greater  $p$ - $d$  hybridization and spatial extent of the  $5d$  states.

Contrariwise, the 12-band  $pp$  hopping processes have larger amplitude in SrVO<sub>3</sub>. Our interpretation is that

in this case, the larger spatial distance prevails; indeed, the difference in Wannier function spread  $\langle r^2 \rangle$  between SrVO<sub>3</sub> and BaOsO<sub>3</sub> is much more pronounced for the  $d$  than for the  $p$  orbitals. The exceptions to this rule,  $t_{p\pi p\pi}^{(1)}$  and  $t_{p\sigma p\sigma}^{(1)}$  (hopping across the octahedron), may be explained by the stronger  $p$ - $d$  hybridization in BaOsO<sub>3</sub>.

- <sup>1</sup> J. G. Bednorz and K. A. Müller, Z. Phys B **64**, 189 (1986); Y. Kamihara, T. Watanabe, M. Hirano, and H. Hosono: J. Am. Chem. Soc. **130**, 3296 (2008).
- <sup>2</sup> P. Coleman, and A. J. Schofield, Nature **433**, 226 (2005).
- <sup>3</sup> V. I. Anisimov, J. Zaanen and O. K. Andersen, Phys. Rev. B **44** 943 (1991).
- <sup>4</sup> V. I. Anisimov, A. I. Poteryaev, M. A. Korotin, A. O. Anokhin and G. Kotliar, J. Phys. Cond. Matter **9** 7359 (1997); A. I. Lichtenstein and M. I. Katsnelson, Phys. Rev. B **57** 6884 (1998); K. Held, I. A. Nekrasov, G. Keller, V. Eyert, N. Blümer, A. McMahan, R. Scalettar, T. Pruschke, V. I. Anisimov and D. Vollhardt, phys. stat. sol. (B) **243** 2599 (2006); G. Kotliar, S. Y. Savrasov, K. Haule, V. S. Oudovenko, O. Parcollet and C. A. Marianetti, Rev. Mod. Phys. **78** 865 (2006); K. Held, Adv. Phys. **56**, 829 (2007).
- <sup>5</sup> G.H. Wannier, Phys. Rev. **52**, 191 (1937).
- <sup>6</sup> E. Müller-Hartmann, Z. Phys. B **74** 507 (1989).
- <sup>7</sup> N. Parragh, G. Sangiovanni, P. Hansmann, S. Hummel, K. Held, and A. Toschi, Phys. Rev. B **88**, 195116 (2013).
- <sup>8</sup> J. C. Slater, *Quantum Theory of Atomic Structure* (McGraw-Hill, New York, 1960); J. S. Griffith, *The Theory of transition-metal ions* (Cambridge University Press, Cambridge, 1971).
- <sup>9</sup> J. Kanamori, Progr. Theor. Phys. **30**, 275 (1963).
- <sup>10</sup> C. J. Ballhausen, *Introduction to Ligand Field theory* (McGraw-Hill, New York, 1962).
- <sup>11</sup> M. W. Haverkort, M. Zwierzycki, and O. K. Andersen, Phys. Rev. B **85**, 165113 (2012); N. Rezaei, P. Hansmann, M. S. Bahrany, R. Arita; Phys. Rev. B **89**, 125125 (2014).
- <sup>12</sup> See, among others, P. Blaha, K. Schwarz, G. Madsen, D. Kvasnicka, J. Luitz, User's Guide, Wien2K\_13.1 [www.wien2k.at/reg\_user/textbooks] Jan Kunes, Alexey V. Lukoyanov, Vladimir I. Anisimov, Richard T. Scalettar, Warren E. Pickett, Nature Materials **7**, 198 (2008); E. Assmann, P. Blaha, R. Laskowski, K. Held, S. Okamoto, and Giorgio Sangiovanni, Phys. Rev. Lett. **110**, 078701 (2013); C. Franchini, R. Kovacik, M. Marsman, S. Sathyanarayana Murthy, J. He, C. Ederer, and G. Kresse, J. Phys.: Condens. Matter **24** 235602 (2012); Tsirlin, Alexander A. and Janson, Oleg and Rosner, Helge, Phys. Rev. B **84**, 144429 (2011); Ylvisaker, Erik R. and Pickett, Warren E. and Koepernik, Klaus, Phys.Rev. B **79**, 035103 (2009).
- <sup>13</sup> In DFT+DMFT usually Kanamori interaction parameters are used, see, among others<sup>35</sup>, K. Haule, C.-H. Yee, and K. Kim, Phys. Rev. B **81**, 195107 (2010); I. Di Marco, P. Thunström, M. I. Katsnelson, J. Sadowski, K. Karlsson, S. Lebègue, J. Kanski, and O. Eriksson, Nature Communications **4**, 2645 (2013); P. Hansmann, A. Toschi, G. Sangiovanni, T. Saha-Dasgupta, S. Lupi, M. Marsi, and K. Held Phys. Status Solidi B **250**, 1251 (2013); S. Backes, D. Guterding, H. O. Jeschke, and R. Valenti, New J. Phys. **16** 083025, (2014); Z. Zhong, M. Wallerberger, J. M. Tomczak, C. Taranto, N. Parragh, A. Toschi, G. Sangiovanni, and K. Held, arXiv:1312.5989; G. Giovannetti, M. Aichhorn, and M. Capone, arXiv:1402.0901. H. T. Dang, X. Ai, A. J. Millis, C. A. Marianetti, arXiv:1407.6505.
- <sup>14</sup> For DFT+DMFT calculations with Slater integrals see, e.g., P. Thunström, I. Di Marco, O. Eriksson, Phys. Rev. Lett. **109**, 186401 (2012); R. Arita, J. Kunes, A.V. Kozhevnikov, A.G. Eguiluz, and M. Imada, Phys. Rev. Lett. **108**, 086403 (2012).
- <sup>15</sup> Note that in constrained random phase approximation<sup>40</sup> one can in principle and sometimes does calculate the full Coulomb interaction matrix. However, usually the subsequent DMFT calculation only employ Slater or Kanamori parameters if not a Kanamori parameterization is assumed from the very beginning.<sup>41?</sup>
- <sup>16</sup> See, e.g., G. F. Koster, J. O. Dimmock, R. G. Wheeler, H. Statz, *Properties of the Thirty-two Point Groups*, MIT Press, Cambridge, Massachusetts, (1963).
- <sup>17</sup> M. Imada, A. Fujimori, and Y. Tokura, Rev. Mod. Phys. **70**, 1039 (1998).
- <sup>18</sup> A. Georges, L. de' Medici, and J. Mravlje, Annual Reviews of Condensed Matter Physics **4**, 137 (2013). S. Sugano, Y. Tanabe, and H. Kamimura, Multiplets of transition-metal ions in crystals, Academic Press (New York) 1970.
- <sup>19</sup> Note that without the  $e_g$  orbitals the Hamiltonian itself is actually not spherically symmetric. Rotation of e.g. the  $d_{xy}$  orbital around the  $z$ -axis maps it onto a linear combination involving (missing)  $e_g$  orbitals; rotating it around the  $x$ - or  $y$ -axis maps it onto a linear combination of the (included)  $t_{2g}$ . The Hamiltonian is invariant under the latter rotations if  $U = U' + 2J$ .



- <sup>20</sup> P. Blaha, K. Schwarz, G. K. H. Madsen, D. Kvasnicka, and J. Luitz, *WIEN2k, An Augmented Plane Wave + Local Orbitals Program for Calculating Crystal Properties* (Techn. Universität Wien, Vienna, Austria, 2001).
- <sup>21</sup> J.P. Perdew, S. Burke, and M. Ernzerhof, *Phys. Rev. Lett.* **77**, 3865 (1996).
- <sup>22</sup> A.A. Mostofi, J.R. Yates, Y.-S. Lee, I. Souza, D. Vanderbilt, and N. Marzari, *Comp. Phys. Commun.* **178**, 685 (2008); N. Marzari, A.A. Mostofi, J.R. Yates, I. Souza, and D. Vanderbilt, *Rev. Mod. Phys.* **84**, 1419 (2012).
- <sup>23</sup> J. Kuneš, R. Arita, P. Wissgott, A. Toschi, H. Ikeda, and K. Held, *Comp. Phys. Commun.* **181**, 1888 (2010).
- <sup>24</sup> A. Sekiyama, H. Fujiwara, S. Imada, S. Suga, H. Eisaki, S. I. Uchida, K. Takegahara, H. Harima, Y. Saitoh, I. A. Nekrasov, G. Keller, D. E. Kondakov, A. V. Kozhevnikov, Th. Pruschke, K. Held, D. Vollhardt and V. I. Anisimov, *Phys. Rev. Lett.* **93** 156402 (2004); E. Pavarini, S. Biermann, A. Poteryaev, A. I. Lichtenstein, A. Georges and O. K. Andersen, *Phys. Rev. Lett.* **92** 176403 (2004); A. Liebsch, *Phys. Rev. Lett.* **90** 096401 (2003); I. A. Nekrasov, G. Keller, D. E. Kondakov, A. V. Kozhevnikov, T. Pruschke, K. Held, D. Vollhardt and V. I. Anisimov, *Phys. Rev. B* **72** 155106 (2005).
- <sup>25</sup> J. M. Tomczak, M. Casula, T. Miyake, F. Aryasetiawan, and S. Biermann *Europhys. Lett.* **100**, 67001 (2012); C. Taranto, M. Kaltak, N. Parragh, G. Sangiovanni, G. Kresse, A. Toschi, and K. Held; *Phys. Rev. B* **88**, 165119 (2013).
- <sup>26</sup> E. Pavarini, A. Yamasaki, J. Nuss, and O.K. Andersen, *New J. Phys.* **7**, 188 (2005).
- <sup>27</sup> A. Scaramucci, J. Ammann, N.A. Spaldin, C. Ederer, *arXiv:1405.3804*
- <sup>28</sup> Y. Shi, Y. Guo, Y. Shirako, W. Yi, X. Wang, A. A. Belik, Y. Matsushita, H. L. Feng, Y. Tsujimoto, M. Arai *et al.* *J. Amer. Chem. Soc.* **135**, 16507 (2013).
- <sup>29</sup> P. Hansmann, N. Parragh, A. Toschi, G. Sangiovanni, and K. Held, *New J. Phys.* **16**, 033009 (2014).
- <sup>30</sup> Z. Zhong, A. Toth, and K. Held, *Phys. Rev. B* **87**, 161102(R) (2013)
- <sup>31</sup> Note that  $t$  in Eq. (5) is  $|t| \sim 2|t_{dp\pi}|$  since the former denotes the hopping between  $d$  and  $O$  orbitals, and the latter between  $d$  and  $p$ .
- <sup>32</sup> We have checked for convergence and errors with respect to the number of Wannierization  $k$ -points, the size of the real space cell, the number of real space support points, and shifts of these support points. The accuracy of integrals is  $\lesssim 0.2\%$ .
- <sup>33</sup> J. Mravlje, M. Aichhorn, T. Miyake, K. Haule, G. Kotliar, and A. Georges, *Phys. Rev. Lett.* **106**, 096401 (2011).
- <sup>34</sup> L. Vaugier, H. Jiang, and Silke Biermann, *Phys. Rev. B* **86**, 165105 (2012)
- <sup>35</sup> L. de' Medici, J. Mravlje, and A. Georges, *Phys. Rev. Lett.* **107**, 256401 (2011); K. Haule and G. Kotliar, *New J. Phys.* **11**, 025021
- <sup>36</sup> Y. C. Lan, X. L. Chen, and A. He, *J. Alloys Compd.* **354**, 95 (2003).
- <sup>37</sup> A. N. Rubtsov and A. I. Lichtenstein, *JETP Lett.* **80** 61 (2004); P. Werner, A. Comanac, L. de' Medici, M. Troyer and A. J. Millis, *Phys. Rev. Lett.* **97** 076405 (2006); E. Gull, P. Werner, O. Parcollet, and M. Troyer, *Eur. Phys. Lett.* **82**, 5700 3 (2008); E. Gull, A. J. Mills, A. I. Lichtenstein, A. N. Rubtsov, M. Troyer, P. Werner, *Rev. Mod. Phys.* **83**, 349 (2011).
- <sup>38</sup> N. Parragh, A. Toschi, K. Held, and G. Sangiovanni, *Phys. Rev. B* **86**, 155158 (2012).
- <sup>39</sup> The signs of the hopping amplitudes reported here are as they would appear in a Hamiltonian matrix, i.e. without the extra sign of “ $-t$ ”.
- <sup>40</sup> F. Aryasetiawan, M. Imada, A. Georges, G. Kotliar, S. Biermann and A. I. Lichtenstein, *Phys. Rev. B* **70**, 195104 (2004); T. Miyake, F. Aryasetiawan, M. Imada, *Phys. Rev. B* **80**, 155134 (2009). M. Hirayama, T. Miyake, M. Imada, *Phys. Rev. B* **87**, 195144 (2013); M. Imada and T. Miyake, *J. Phys. Soc. Jpn.* **79**, 112001 (2010).
- <sup>41</sup> M. Hirayama, T. Miyake, M. Imada, *Phys. Rev. B* **87**, 195144 (2013).